

# A Numerical Method for Calculating Transmission Coefficients Across Arbitrary Potential Barriers with High Accuracy

Ding Wuchang<sup>†</sup>, Xu Xuejun, Cheng Buwen, Zuo Yuhua, Yu Jinzhong, and Wang Qiming

(State Key Laboratory of Integrated Optoelectronics, Institute of Semiconductors,  
Chinese Academy of Sciences, Beijing 100083, China)

**Abstract:** We report a new method for calculating transmission coefficients across arbitrary potential barriers based on the Runge-Kutta method. A numerical solution of the Schrödinger equation is calculated using the Runge-Kutta method, and a new model is established to analyze the numerical results to find the transmission coefficient. This technique is applied to various cases, such as parabolic potential barrier and double-barrier structures. Transmission probability with high precision is obtained and discussed. The tunnelling current density through a MOS structure is also explored and the result coincides with the Fowler-Nordheim model, which indicates the applicability of our method.

**Key words:** transmission coefficient; tunneling probability; Runge-Kutta method

**PACC:** 0365; 7335C

**CLC number:** O471.1

**Document code:** A

**Article ID:** 0253-4177(2008)02-0201-05

## 1 Introduction

With recent advances in the fabrication of semiconductor quantum structures, the tunnelling effect deserves attention because of its key role in devices such as light emitting devices with MOS structures based on silicon<sup>[1,2]</sup>. In order to understand the physical properties of these devices, the transmission coefficient has to be investigated. For decades, several methods have been developed for calculating the transmission coefficient. The WKB approximation method is the most conventional method for most cases. However, it is not suitable for some complicated cases because its accuracy is insufficient. The transfer-matrix method has been widely used for studying quantum structures and methods based on transfer-matrix method have been developed<sup>[3~7]</sup>. However, there are also limitations on these methods, such as the continuous turning points problem, which is encountered when a continuous potential energy equals the energy of the tunnelling particle. Many other methods, like the Monte Carlo method and the finite element method, are complicated to implement.

In this paper, we report a numerical method to calculate transmission coefficients across arbitrary potential barriers in the one dimensional case. A numerical solution of the Schrödinger equation based on the Runge-Kutta method<sup>[8]</sup> is obtained, and the transmission coefficient is deduced from analysis of the numerical solution by applying our new model. This

method can be easily used for any potential distribution and the results are credible with high accuracy.

## 2 Theory

The time-independent Schrödinger equation in one dimension is given by

$$\left[ -\frac{d}{dx} \frac{\hbar^2}{2m(x)} \frac{d}{dx} + V(x) \right] \Psi(x) = E\Psi(x) \quad (1)$$

where  $m(x)$  is the effective mass of the particle,  $V(x)$  is the potential energy variation, and  $E$  and  $\Psi(x)$  represent the energy and wave function, respectively. The Runge-Kutta method<sup>[8]</sup> is used to calculate the numerical solution. In this case, Equation (1) is changed into first order equations,

$$\frac{d}{dx} \Psi(x) = y(x) \quad (2)$$

$$\left[ -\frac{d}{dx} \frac{\hbar^2}{2m(x)} y(x) + V(x) \right] \Psi(x) = E\Psi(x) \quad (3)$$

Given the value of  $\Psi(x)$  and  $y(x)$  at a specified position, we can get the value of  $\Psi(x)$  everywhere by using the Runge-Kutta method.

Consider a potential barrier with an arbitrary potential distribution in the middle region, but with constant potential on both sides, in other words,

$$V(x) = \begin{cases} V_1, & x \leq x_1 \\ \text{Arbitrary value}, & x_1 < x < x_2 \\ V_3, & x \geq x_2 \end{cases}$$

where  $V_1$  and  $V_3$  are constants and can be different, as shown in Fig. 1. If the particle is tunneling from the left and the transmitted wave is a unit amplitude plane wave, the wave function can be described as

<sup>†</sup> Corresponding author. Email: wcd04@semi.ac.cn

Received 4 September 2007, revised manuscript received 8 October 2007

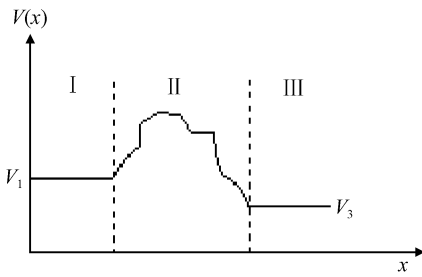


Fig. 1 Schematic representation of the potential barrier being investigated

$$\Psi_I = a \exp[i(k_1 x + \varphi_1)] + b \exp[-i(k_1 x + \varphi_3)] \quad (4)$$

$$\Psi_{III} = \exp[i(k_3 x)] \quad (5)$$

where  $\Psi_I$  and  $\Psi_{III}$  are the wave functions in regions I and III respectively, and  $a$  and  $b$  represent the amplitude coefficients to be determined.  $k_1 = \sqrt{2m_1^*(E - V_1)}/\hbar$ ,  $k_3 = \sqrt{2m_3^*(E - V_3)}/\hbar$ ,  $m_1^*$  and  $m_3^*$  are the particle's effective mass in regions I and III. The real and imaginary part of  $\Psi_I$  can be obtained from Eq. (4), which are:

$$\begin{aligned} \text{Re}(\Psi_I) &= \sqrt{[a + b \cos(\Delta\varphi)]^2 + b^2 \sin^2(\Delta\varphi)} \\ &\quad \sin(k_3 x + \varphi_1 + \varphi_{p1}) \\ \text{Im}(\Psi_I) &= \sqrt{[a - b \cos(\Delta\varphi)]^2 + b^2 \sin^2(\Delta\varphi)} \\ &\quad \sin(k_3 x + \varphi_1 + \varphi_{p2}) \end{aligned} \quad (6)$$

where

$$\begin{aligned} \varphi_{p1} &= \tan^{-1} \left( -\frac{a + b \cos(\Delta\varphi)}{b \sin(\Delta\varphi)} \right) \\ \varphi_{p2} &= \tan^{-1} \left( -\frac{b \sin(\Delta\varphi)}{a - b \cos(\Delta\varphi)} \right) \end{aligned}$$

and  $\Delta\varphi = \varphi_2 - \varphi_1$ . On the other hand, with the initial condition in region III, which can be easily decided according to Eq. (5), the wave function values can be deduced by the Runge-Kutta method. Thus, the amplitudes of the real and imaginary part of  $\Psi_I$  are definitely described as

$$\sqrt{[a + b \cos(\Delta\varphi)]^2 + b^2 \sin^2(\Delta\varphi)} = A_{re} \quad (7)$$

$$\sqrt{[a - b \cos(\Delta\varphi)]^2 + b^2 \sin^2(\Delta\varphi)} = A_{im} \quad (8)$$

where  $A_{re}$  and  $A_{im}$  are the numerical values deduced from fitting the values of the wave function in region I with sine functions. Meanwhile the phase information of the wave function is also obtained from numerical calculation, but we do not take it into account because a little deviation of the phase leads to huge mistakes. The probability conservation law is used instead to determine the transmission coefficient,

$$\frac{\hbar k_1}{m_1^*} (a^2 - b^2) = \frac{\hbar k_3}{m_3^*} \quad (9)$$

By solving Eqs. (7)~(9), we obtain the amplitude of the incident wave,  $a$ . Thus, the transmission coefficient is obtained as

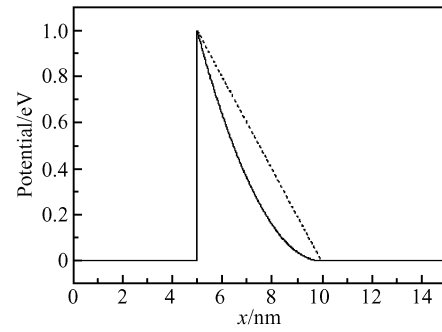


Fig. 2 Schematic representation of the potential distribution. The dotted curve refers to  $n = 1$  and the solid curve refers to  $n = 2$ .

$$T = \frac{k_3 m_1^*}{k_1 m_3^*} \times \frac{1}{|a|^2}$$

### 3 Applications

In this section we first apply our method to a parabolic potential distribution. The parabolic potential is widely encountered in heterostructures, metal-semiconductor contacts, and MIS structures, etc. Methods have been developed to deal with different cases<sup>[7,9]</sup>. For general consideration, the following case is investigated,

$$V(x) = \begin{cases} V_0 \left( \frac{a-x}{a} \right)^n, & 0 \leq x < a \\ 0, & \text{others} \end{cases} \quad (10)$$

where  $V_0$  is the height of the potential barrier and  $a$  represents the barrier width, which is illustrated in Fig. 2. For the parabolic potential barrier,  $n = 2$ . Sometimes a linear potential barrier is considered for an approximation, where  $n = 1$ , and in this case other methods can be applied such as Airy's function based methods. We have calculated the transmission coefficient of the two cases and compared the differences between them.

For numerical calculation,  $V_0 = 1\text{eV}$  and  $a = 5\text{nm}$ . The tunnelling particle is an electron with an effective mass of  $m_0 = 9.1 \times 10^{-31}\text{kg}$ . Transmission coefficients are shown in Fig. 3. It is hard for an electron with energy below  $0.8\text{eV}$  to pass through the potential barrier. After the electron energy reaches  $0.8\text{eV}$ , the transmission coefficient increases rapidly. While having little difference between the two cases, the transmission coefficient through the parabolic potential barrier is always larger than that of the linear case because the integration of the parabolic potential is smaller. Another interesting feature is the oscillatory behavior of the linear potential case, which is shown in the inset of Fig. 3. This behavior is due to quantum mechanical reflection, which is similar to the

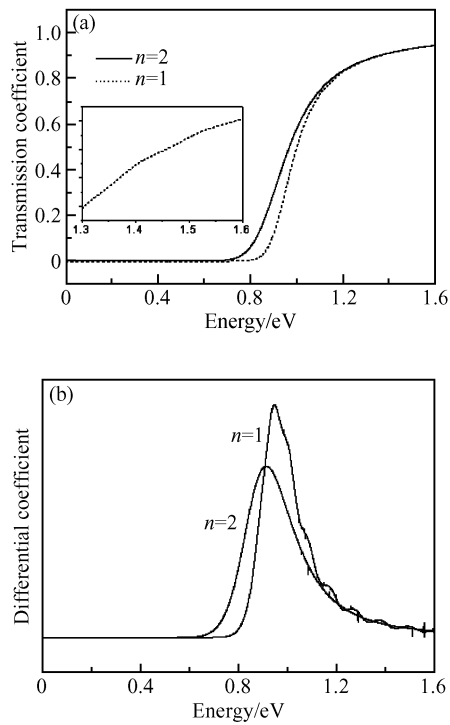


Fig.3 (a) Transmission coefficient as a function of the incident electron energy for the potential in Fig. 1; (b) Differential coefficient of the two curves in Fig.3 (a)

rectangle barrier ( $n = 0$ ). But in the parabolic potential case, this behavior fades away and the curve is totally smooth. We confirmed this by calculating the differential coefficient, which is also shown in Fig. 3. The abrupt fluctuations are due to miscalculation. However, we are not sure if  $n = 2$  is the critical point at which the oscillatory behavior disappears.

Double-barrier resonant tunneling nanostructures have attracted great research interest because of their potential for device applications, and their significance in study of the physics of confined structures. The physics of resonant tunneling in symmetric double barrier systems is well understood. Asymmetric systems, especially in the presence of a constant field, have also been widely investigated. In this work, we calculate the transmission coefficient for an incident electron in double-barrier systems, and compare our results with those of Allen *et al.* [9] to show the applicability of our method. We therefore make calculations on the same structures in Ref. [9], which is illustrated in Fig. 4.

Table 1 Parameters for calculation

	$V_a/eV$	$U_B/eV$	$U_D/eV$	$b/nm$	$c/nm$	$d/nm$
Curve 1	0.16	0.5	0.5	2	5	2
Curve 2	0.16	0.5	0.5	2	5	4
Curve 3	0.16	0.5	0.5	4	5	2
Curve 4	0.16	0.5	0.5	2	5	3

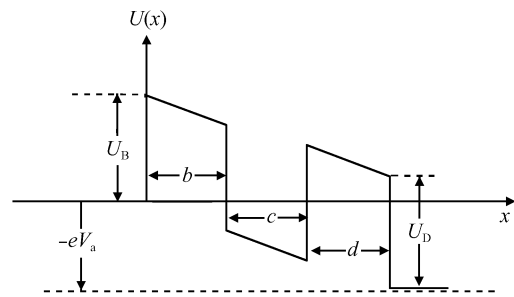


Fig.4 Schematic representation of potential distribution [8]

Figure 5 (a) shows the transmission coefficient  $\ln T$  and the parameters are listed in Table 1. The effective mass of the electron is  $0.1087m_0$  in the barrier region and  $0.067m_0$  elsewhere. In Allen's work, a problem due to use of exact Airy functions is encountered when the incident electron energy is very low, and a resonance in the low energy region has been declared but not obtained. Our method overcomes this problem and achieves extremely accurate results in the low energy region. Indeed, there are two resonances for each curve, which indicates that there are two quasi-bound states in the quantum wells. For curve 2, the first resonant peak is much sharper than other curves. In this case, the width of the second barrier ( $d = 4nm$ ) is thicker, so it is hard for an electron to escape from the well, giving the electron a long lifetime and narrowing the width of the quasi-bound state.

Comparing curves 2 and 1, we find although the second peak of curve 2 is higher, the first peak is opposite. Therefore, we do not think this is a sufficient

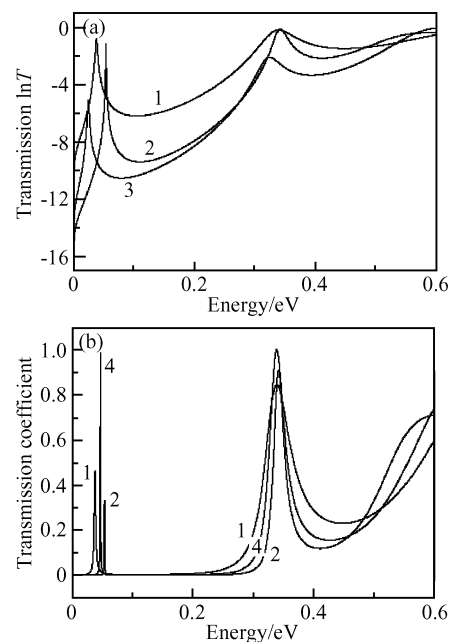


Fig.5 Transmission coefficient as a function of incident electron energy for double barrier structures The parameters are listed in Table 1.

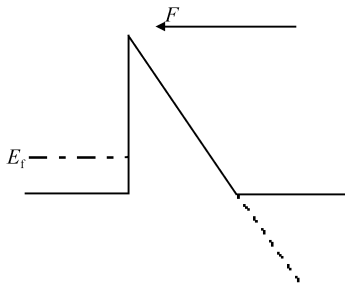


Fig. 6 Potential distribution for a MOS structure simulation  $F$  represents the electric field.

proof for Mendez's concept of an effective-barrier symmetry<sup>[3]</sup>. In order to find a more appropriate application of this concept, we have considered some other situations. When  $d = 3\text{nm}$  (curve 4), both peaks are higher than those of curve 1 and the peak values are close to 1 as shown in Fig. 5 (b). This case may be a more credible certification of Mendez's concept.

We have also applied our method to MOS structures. In recent years, light emitting devices based on silicon have attracted much attention due to their prospective application in optical integration. Several research groups have reported the light emitting devices based on silicon with MOS structures in which the tunneling effect is a key factor<sup>[1,2]</sup>. For technical study, the tunnel current through a linearly varying potential has been calculated. In order to use our model, the potential configuration is modified as shown in Fig. 6. The barrier height is  $1.0\text{eV}$ , and Fermi level of the incident side is  $E_f = 0.3\text{eV}$ . The effective mass is considered to be  $m_0 = 9.1 \times 10^{-31}\text{kg}$  everywhere.

To avoid infinite integration, the temperature is fixed at  $0\text{K}$ . Thus, the current density can be deduced from:

$$J = \frac{em^*}{2\pi^2\hbar^3} \int_0^{E_f} dE_{\perp} (E_f - E_{\perp}) T(E_{\perp}) \quad (12)$$

where  $E_{\perp}$  represents the vertical part of the incident energy to the interface. The relationship of the tunneling current density and the applied electric field is shown in Fig. 7. We can clearly find:

$$J \propto AF^2 \exp\left(-\frac{B}{F}\right) \quad (13)$$

which is the well-known Fowler-Nordheim tunneling effect. Fowler-Nordheim tunnelling is a critical injection process for some light emitting devices<sup>[2]</sup>. These results indicate the accuracy and possible application of our method.

## 4 Conclusion

In conclusion, we have presented a new method for calculating transmission coefficient by using a

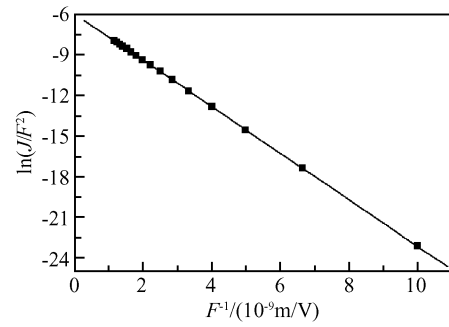


Fig. 7 Relationship of tunnelling current and the applied electric field for the potential distribution in Fig. 6 The line is a guideline for eyes.

Runge-Kutta method to solve the Schrödinger equation and we analyzed the numerical results. Arbitrary potential distribution with constant sides can be treated by this method and the results are quite accurate. Tunnelling probability through a parabolic potential barrier is obtained and discussed. A double barrier case is investigated and the results show some detailed features in addition to partial agreement with conclusions deduced from other methods. A modified MOS structure is also surveyed and the results agree with the Fowler-Nordheim tunneling model. All these calculations show the applicability and accuracy of our method, which is expected to be explored for further application.

## References

- [1] Nazarov A, Sun J M, Skorupa W, et al. Light emission and charge trapping in Er-doped silicon dioxide films containing silicon nanocrystals. *Appl Phys Lett*, 2005, 86: 151914
- [2] Jambois O, Garrido B, Pellegrino P, et al. White electroluminescence from C- and Si-rich thin silicon oxides. *Appl Phys Lett*, 2006, 89: 253124
- [3] Wang H M, Zhang Y F. Airy function and transfer matrix method in the study of quasi-bound levels of biased multi-barrier quantum structures. *Acta Phys Sin*, 2005, 54: 2226
- [4] Ricco B, Azbel M Y. Physics of resonant tunneling: the one-dimensional double-barrier case. *Phys Rev B*, 1984, 29: 1970
- [5] Ghatak A K, Thyagarajan K, Shenoy M R. A novel numerical technique for solving one-dimensional Schrödinger equation using matrix approach — application to quantum well structures. *IEEE J Quantum Electron*, 1988, 24: 1524
- [6] Jonsson B, Eng S T. Solving the Schrödinger equation in arbitrary quantum-well potential profiles using the transfer matrix method. *IEEE J Quantum Electron*, 1990, 26: 2025
- [7] He Y, Cao Z Q, Shen Q S. Analytical formula of the transmission probabilities across arbitrary potential barriers. *J Phy A: Math Gen*, 2005, 38: 5771
- [8] Dormand J R, Prince P J. A family of embedded Runge-Kutta formulae. *J Comp Appl Math*, 1980, 6: 19
- [9] Gong J, Liang X X, Ban S L. Resonant tunnelling in parabolic quantum well structures under a uniform transverse magnetic field. *Chin Phys*, 2005, 14: 0201
- [10] Allen S S, Richardson S L. Theoretical investigations of resonant tunneling in asymmetric multibarrier semiconductor heterostructures in an applied constant field. *Phys Rev B*, 1994, 50: 11693

## 任意势垒隧穿几率的一种高精度数值算法

丁武昌<sup>†</sup> 徐学俊 成步文 左玉华 余金中 王启明

(中国科学院半导体研究所 光电集成实验室, 北京 100083)

**摘要:** 基于龙格-库塔算法求解薛定谔方程, 并对获得的数值结果进行分析得出精确的量子隧穿几率. 通过适当的处理, 该方法适用于任意势垒的情形. 利用该方法计算了多种结构的隧穿几率, 如抛物线型势垒及双势垒, 获得了高精度的隧穿几率. 同时计算了 MOS 结构的隧穿电流密度, 结果与 Fowler-Nordheim 隧穿完全吻合, 表明了该方法的适用性.

**关键词:** 隧穿系数; 隧穿几率; 龙格-库塔法

**PACC:** 0365; 7335C

**中图分类号:** O471.1

**文献标识码:** A

**文章编号:** 0253-4177(2008)02-0201-05

<sup>†</sup> 通信作者. Email: wcd04@semi.ac.cn

2007-09-04 收到, 2007-10-08 定稿